

Rotating states for trapped bosons in an optical lattice

EMIL LUNDH

Department of Physics, Umeå University, SE-90187 Umeå, Sweden

PACS 03.75.Lm – Tunneling, Josephson effect, Bose-Einstein condensates in periodic potentials, solitons, vortices, and topological excitations

Abstract. - Rotational states for trapped bosons in an optical lattice are studied in the framework of the Hubbard model. Critical frequencies are calculated and the main parameter regimes are identified. Transitions are observed from edge superfluids to vortex lattices with Mott insulating cores, and subsequently to lattices of interstitial vortices. The former transition coincides with the Mott transition. Changes in symmetry of the vortex lattices are observed as a function of lattice depth. Predictions for experimental signatures are presented.

Ultracold atoms in optical lattices combined with trapping potentials offer rich possibilities for exploring new physics. In particular, the presence of a trap allows for the coexistence of phases such as the Mott insulator and superfluid, as was predicted by Jaksch *et al.* [1], realized by Greiner *et al.* [2], and directly verified by two independent groups in 2006 [3, 4]. The harmonic confinement results in a shell-like structure, where superfluid and Mott insulating regions occupy alternating intervals (in one dimension), annuli (in two dimensions), or spherical shells (in three dimensions).

Motivated by the progress in the study of vortex physics in trapped condensates, rotational states in optical lattices have attracted some recent attention. At one end of the rich spectrum of possibilities is the case of a weak periodic potential that acts as a lattice of pinning centers for vortices; this has been realized in experiment using a corotating periodic potential [5, 6]. For deeper optical lattices, one may consider a discretized description of the gas, the bosonic Hubbard model [1, 7], and study how rotational states interact with the quantum phases of the model. It has been predicted that quantized vortices in the Hubbard model possess a Mott insulating core [8, 9], and also that in the limit of a deep lattice, rotational states appear as an edge superfluid surrounding a Mott insulator [10]. In the limit of rapid rotation, when the number of vortices is comparable to the number of lattice sites, intriguing phenomena are predicted such as strongly correlated vortex liquids [11] and fractal densities of states, the so-called Hofstadter butterfly [9, 12–14].

This study aims to investigate the interplay between the quantum phase transition, rotation, and trapping for

atoms in an optical lattice described by the bosonic Hubbard model, and to describe the different types of rotational state that can be found in such a system. It will be seen that at moderate rotational velocities, the rotational states of the system are closely connected to the Mott transition. Since much of the qualitative physics is expected to be brought out already in two dimensions, the study is carried out in 2D.

A gas of spinless bosonic atoms in an optical lattice is known to be well described by the Hubbard model [1]. In the presence of rotation, the Hamiltonian is [8, 10]

$$H - \Omega L_z - \mu N = -t \sum_{\langle ij \rangle} a_i^\dagger a_j e^{-i\phi_{ij}} + \frac{U}{2} \sum_i a_i^\dagger a_i^\dagger a_i a_i + \sum_i \left[\frac{1}{2} (\tilde{\omega}^2 - \tilde{\Omega}^2) r_i^2 - \mu \right] a_i^\dagger a_i, \quad (1)$$

where i, j label the lattice sites, $\langle ij \rangle$ denotes nearest neighbors, and \mathbf{r}_i is the position vector of site i with length r_i . U is the on-site interaction strength, t is the tunneling matrix element, and μ is the chemical potential. The rotation introduces a phase ϕ_{ij} . An alternative Hamiltonian was proposed in Ref. [7] using a corotating ansatz for the single-particle orbitals; however, the quantitative differences would be exceedingly small in the present case. We state energies in units of the recoil energy E_R and distances in units of the lattice constant $d = \lambda/2$ where λ is the wavelength of the lattice beams, and for definiteness the Wannier functions are approximated by Gaussians. In this approximation $t = V_0^{3/4} \pi^{5/4} [1 - (2/\pi)^2] \exp(-\pi^{3/2} \sqrt{V_0}/4)/4$, and $U = V_0^{3/4} a/\sqrt{2}$, where V_0 is the depth of the lattice potential and a is the s -wave scattering length of the atoms.

For the calculations, we have assumed ^{87}Rb atoms with a scattering length $a = 5.77\text{nm}$ and a square lattice made out of two pairs of counterpropagating beams with wavelength $\lambda = 780\text{nm}$. We define $\tilde{\Omega} = \pi\hbar\Omega/\sqrt{2}$, where Ω is the rotational frequency, and $\tilde{\omega} = \pi\hbar\omega/\sqrt{2}$, where ω is the frequency of the harmonic magnetic trapping potential. Finally, the phase $\phi_{ij} = (m/\hbar) \int_{\mathbf{r}_i}^{\mathbf{r}_j} d\mathbf{r} \cdot (\mathbf{\Omega} \times \mathbf{r})$, where in this 2D study the vector $\mathbf{\Omega}$ points out of the plane.

The Hamiltonian in Eq. (1) describes an optical lattice that rotates with the frequency Ω . Such a potential was realized in Ref. [6]. Other ideas for creating a rotating state in an optical lattice include exciting the desired vorticity in a trapped condensate, and applying the optical lattice afterwards. Alternatively, one may stir the gas by using a time-dependent optical or magnetic potential [15], or by phase engineering [16–18], in the presence of a static optical lattice potential. However, the latter options are, rigorously speaking, not described by the Hamiltonian in Eq. (1).

We now map out the rotational phases of the trapped system. The large number of parameters makes for a rich phase diagram. The rotation with frequency Ω gives rise to a centrifugal potential that competes with the confining potential. At the critical value $\Omega = \omega$, the centrifugal potential balances the trap potential, and thus this criterion gives the upper bound for the angular velocity. However, the present method of calculation is not reliable in the fast rotating limit, so we will only consider the regime well away from this upper bound. In addition, we work with a rather weak trapping potential, $\tilde{\omega} = 0.025$, and hence the scaled rotational frequency $\tilde{\Omega}$ must be equally weak. Invoking the analogy with a system in a magnetic field, $\tilde{\Omega}$ is the flux through each plaquette [19]. Thus, the present study takes place in the limit of weak flux, precluding effects such as Hofstadter-butterfly physics [9, 12–14]. However, this limit exhibits a number of interesting physical effects connected with the Mott transition, which will be the subject of the present paper. Furthermore, we deal only with moderate densities, keeping the chemical potential $\mu = 0.5U$ for the most part and increasing it to maximally $\mu = 2.0U$. In this way we can focus on vortex-lattice physics without invoking unnecessary complications such as alternating Mott and superfluid shells. Thus, at fixed $\tilde{\omega}$, we now explore the parameter space spanned by moderate ranges of V_0 , $\tilde{\Omega}$, and μ .

In the absence of rotation and external potential, the Hamiltonian (1) undergoes a quantum phase transition between two types of ground state at a critical value of the ratio of the tunneling and interaction parameters, t/U , depending on the chemical potential μ [20]. When the ratio t/U is large enough, there is phase coherence over the entire sample which puts the system in its superfluid state, and a Bose-Einstein condensate is formed. For weaker tunneling, phase coherence is lost, number fluctuations are suppressed, and the number of atoms per site is locked to an integer. This is the Mott insulating state. The critical tunneling in two dimensions at unit filling was in Ref. [21]

calculated to be $(t/U)_c = 0.060$, while in the mean field approximation, which we shall use here, one finds the lower value $(t/U)_c = 0.042$. In a trapping potential $V(r)$, superfluids and Mott insulators coexist in spatially separated regions, where the local phase is determined by the local chemical potential $\mu_{loc} = \mu - V(r)$ [1, 3, 22]. The size of the regions depends on the ratio t/U , such that for large enough t/U , the whole sample is superfluid, and as t/U decreases, the Mott insulating regions grow.

If the atoms are set into rotation, it is the superfluid fraction that rotates since the Mott fraction is insulating. A continuous superfluid, or a trapped Bose-Einstein condensate in the absence of an optical lattice, responds to rotation by forming a lattice of quantized vortices with hollow cores [23]. There exist excited states confined to the cores, but in a weakly interacting sample their population is modest [24]. In a numerical study of an extended Hubbard model, with interactions between nearest neighbors, it was found that the superfluid forms vortices, and the cores are Mott insulating [8]. In other parameter regimes, interstitial vortices may form, with only modest suppression of the condensate density [9, 11, 13]. Yet another parameter regime was investigated in Ref. [10]. If almost all of the sample is Mott insulating, rotation will result in an edge superfluid containing only a few rotating atoms, and the bulk is unaffected.

Numerical calculations have been carried out on a 100×100 lattice in the mean-field Gutzwiller approximation, which has proven to be reliable in a range of situations [1, 25, 26]. To solve for the rotating states, a phase winding has been imposed onto the nonrotating solution whereafter the energy has been minimized using a conjugate gradient method [10]. 5 single-particle states per lattice site were allowed for in the calculations. Solutions for the case of two phase singularities, i.e., a total phase winding of 4π around the circumference of the sample, are shown in Fig. 1. The Gutzwiller approximation allows for direct calculation of the condensate wavefunction $z_i = \langle a_i \rangle$ at each point; its square $n_{C_i} = |z_i|^2$ is denoted the dimensionless condensate density and is plotted alongside the dimensionless density, which is defined as the mean number of atoms on the site, $n_i = \langle a_i^\dagger a_i \rangle$. The chemical potential is chosen as $\mu = 0.5U$. The mean-field critical point for the Mott transition at $t/U = 0.042$ corresponds to $V_0 = 27.2$. At $V_0 = 26.2$, the entire system is in the superfluid state, and the condensate density is nonzero but contains two depressions which coincide with phase singularities; these are vortices. At these points, the total density is unity, supporting the conclusion of Ref. [8] that the cores are filled with Mott insulating atoms. As V_0 is increased, the condensate density in the center decreases and the edge-superfluid state is entered. At the Mott transition point $V_0 = 27.2$, the condensate density in the center is $n_{C0} = 3.2 \cdot 10^{-6}$, and the two phase singularities are separated by a single lattice site. For larger V_0 , n_{C0} vanishes to within numerical precision close to the center, so that the phase varies erratically. Clearly, the Mott transition

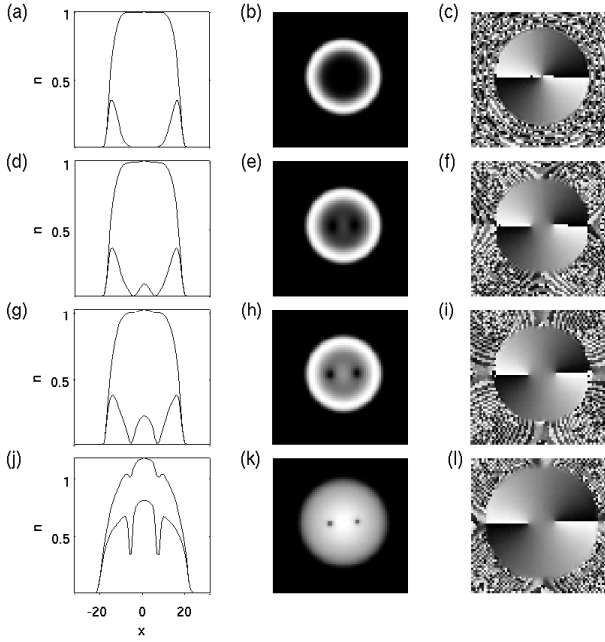


Fig. 1: Density and phase profiles for a system containing two phase singularities, as the Mott transition is crossed. (a), (d), (g), (j): Cross-section at $y = 0$ of the dimensionless density n_i (upper curves) and condensate density n_{Ci} (lower curves). (b), (e), (h), (k): Condensate density. Bright shades signify high density and vice versa. (c), (f), (i), (l): Phase of the condensate wavefunction z_i , increasing with brightness from 0 (black) to 2π (white). The lattice potential height is chosen as $V_0 = 27.2$ (a-c); $V_0 = 26.7$ (d-f); $V_0 = 26.2$ (g-i); and $V_0 = 22$ (j-l). This corresponds to $t/U = 0.0418, 0.0447, 0.0478,$ and 0.0868 , respectively. The chemical potential is $\mu = 0.5U$ and the trapping frequency is $\tilde{\omega} = 0.025$. The rotating frequency is $\tilde{\Omega} = 0.47\tilde{\omega}$ in (a-i) and $\tilde{\Omega} = 0.63\tilde{\omega}$ in (j-l).

is accompanied by a transition between the two types of rotational state.

Since the Mott transition is second order, there is no surface tension associated with the phase boundary and hence no tendency for the vortices to stick together and form giant vortices. In the absence of a lattice potential, a giant vortex is never stable in a harmonic trap [27], and apparently, the same holds for the trapped Hubbard model, as long as the whole system is in the superfluid phase.

Moving further from the Mott transition, i.e., decreasing the lattice depth, the vortex cores are observed to decrease in size. When a vortex core is smaller than the lattice constant, one enters the regime of interstitial vortices, where the depletion of the condensate is modest. An example is shown in Fig. 1(j-l). The reason is that this system is discrete, and the vortices naturally tend to form in the interstices, just as observed in most lattice models. In other words, on a plaquette of 2×2 lattice sites the phase may wind by 2π , and the condensate density does not have to vanish on the sites because the phase singularity is in the

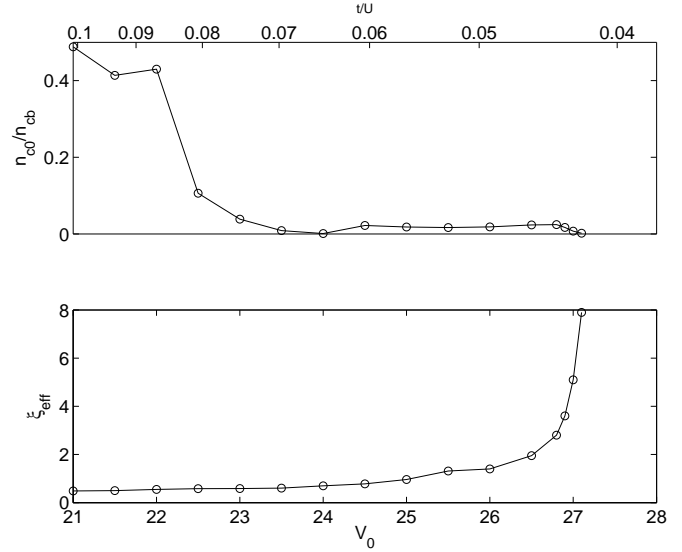


Fig. 2: (a) Size ξ_{eff} of a vortex core as the lattice depth V_0 , and hence the tunneling over on-site energy, t/U , is varied. (b) Ratio of core to bulk condensate density, n_{C0}/n_{Cb} , as a function of V_0 and t/U . The chemical potential is $\mu = 0.5U$, the trapping frequency $\tilde{\omega} = 0.025$, and the rotational frequency is $\tilde{\Omega} = 0.5\tilde{\omega}$.

void between them. A discernible vortex core forms when the balance between the interaction energy and the centrifugal energy is such that a large vortex core is favored. In a trapped Bose-Einstein condensate, the size of a vortex core is given by the healing length, $\xi = \sqrt{t/(Un_{Cb})}$, where n_{Cb} is the mean condensate density away from the vortex [23]. In the vicinity of the Mott transition, the formula cannot be trusted quantitatively, but the dependence on n_{Cb} provides a qualitative explanation of why the vortex core size decreases when one moves away from the Mott transition.

The size of the core of a single vortex has been calculated by fitting the central part of the condensate density profile n_{Ci} to the interpolation formula [23, 28]

$$n_{Ci} = n_{Cb} \frac{(i_x - i_{x0})^2 + (i_y - i_{y0})^2}{(i_x - i_{x0})^2 + (i_y - i_{y0})^2 + \xi_{eff}^2}, \quad (2)$$

where $i = (i_x, i_y)$ is the Cartesian coordinate of a lattice site and i_{x0}, i_{y0} is the location of the center of the vortex. Two series of calculations are made, one where the chemical potential is fixed at $\mu = 0.5U$ and the lattice depth is varied; and one where μ is varied with the lattice depth fixed at $V_0 = 25$. The results for n_{C0} and ξ_{eff} as functions of t/U is shown in Fig. 2, and as functions of μ in Fig. 3.

For simplicity, the angular frequency has been fixed at $\tilde{\Omega} = 0.5\tilde{\omega}$, although the central singly quantized vortex is not the global energy minimum over the whole range.

The crossover from Mott-core vortices to interstitial vortices is most clearly seen in Fig. 2(a), where the condensate density in the vortex core n_{C0} is recorded. In the Mott phase i.e., for $t/U < 0.042$, the condensate den-

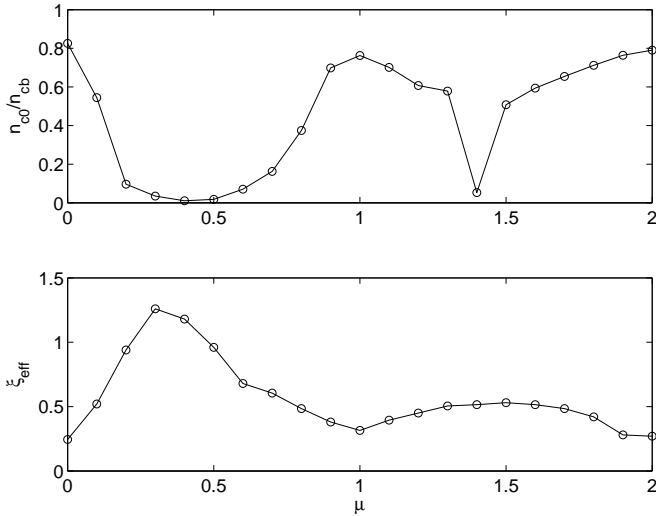


Fig. 3: (a) Size ξ_{eff} of a vortex core as a function of chemical potential μ . (b) Ratio of core to bulk condensate density, n_{C0}/n_{Cb} , as a function of μ . The lattice depth is kept at $V_0 = 25E_R$, which implies $t/U = 0.0564$, the trapping frequency $\tilde{\omega} = 0.025$, and the rotational frequency is $\Omega = 0.5\tilde{\omega}$.

sity in the center is zero to within numerical accuracy. As soon as the superfluid phase is entered, n_{C0} increases to a small but finite value. However, there is a second, reasonably sharp transition, where n_{C0} abruptly rises to a value of about half the condensate density outside the core. This transition is seen to occur when the fit parameter ξ_{eff} has dropped to a value well below one lattice site. The abrupt transition suggests that we can regard the interstitial vortices and Mott-core vortices as distinct rotational phases. In Ref. [9], a homogeneous system with periodic boundary conditions and a large vortex density was studied. A similar abrupt transition was found there between vortices centered on sites and vortices centered on plaquettes. However, as was noted in Ref. [9], since energy differences between different types of ground state may be small close to the Mott transition, it may very well be that the exact phase diagram is substantially different from that presented here.

In Fig. 3, the slightly oscillatory dependency of n_{C0} as a function of μ reflects the proximity in phase space to an alternating sequence of Mott insulating regions centered around $\mu = 0.5, 1.5$, etc. [20, 22]. It is clearly seen that away from the Mott transition, the core size ξ_{eff} decreases and the condensate density in the core n_{C0} jumps to a value of the same order as the bulk condensate density, but close to the Mott insulating regions it is significantly suppressed.

As the angular velocity is increased, the minimum-energy state of the system contains an increasing number of vortices. In Fig. 4 minimum-energy configurations with six phase singularities are plotted far from and close to the Mott transition. In the superfluid phase, a rudimen-

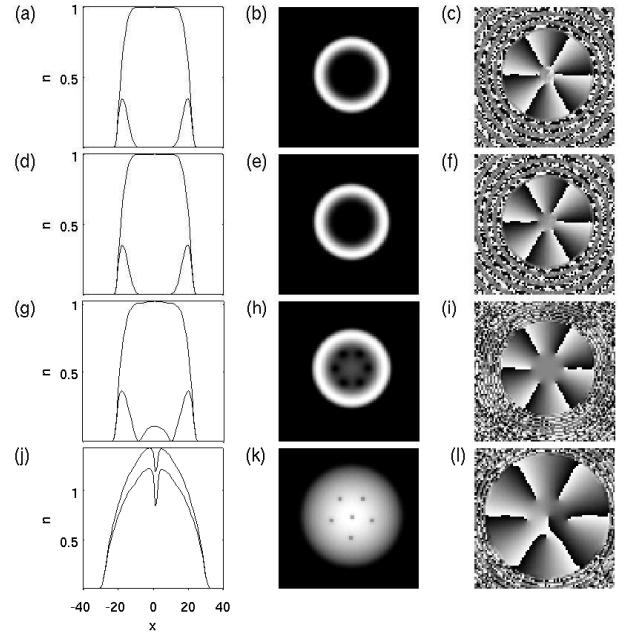


Fig. 4: Density and phase profiles for a system with six phase singularities. The quantities displayed are as in Fig. 1. (a-c): $V_0 = 27.4$, $\Omega/\omega = 0.68$, $t/U = 0.0407$. (d-f): $V_0 = 27.2$, $\Omega/\omega = 0.68$, $t/U = 0.0418$. (g-i): $V_0 = 26.7$, $\Omega/\omega = 0.70$, $t/U = 0.0447$. (j-l): $V_0 = 20$, $\Omega/\omega = 0.77$, $t/U = 0.1176$. The chemical potential is $\mu = 0.5U$. Note that the parameters are slightly different from those in Fig. 1.

tary vortex lattice is formed, resembling those found in trapped condensates (as well as superconductors and liquid helium, of course). The vortices are filled with Mott insulating atoms so that the total density profile is not strongly affected. It is seen that the lattice changes from fivefold to sixfold symmetry for $V_0 > 22$; this is further discussed below. At the Mott transition, $V_0 = 27.2$, the phase singularities do not seem to have molten together – the shortest distance is about 5 lattice sites – but the central density is $n_{C0} = 8 \cdot 10^{-6}$, and as V_0 is further increased, the phase begins to vary erratically in the center, as seen in Fig. 4(c). The figure supports the conclusion that the Mott transition marks the transition between a vortex-lattice state and an edge superfluid. The rotating force does not seem to shift the critical point at least for the rather modest values of Ω considered here.

The critical frequencies $\Omega_{C,q}$ for the thermodynamic stability of a state containing q phase singularities is calculated by comparing the energies of different stationary solutions of the Hamiltonian (1), computed by choosing different phase windings as the initial condition for the energy minimization. The result for the lowest values of q is shown in Fig. 5. It is known from trapped Bose-Einstein condensates that the critical frequency does not directly decide whether a rotating state can be created, since that creation depends on stability properties of surface excitations [29]. For a complete picture, the phase diagram

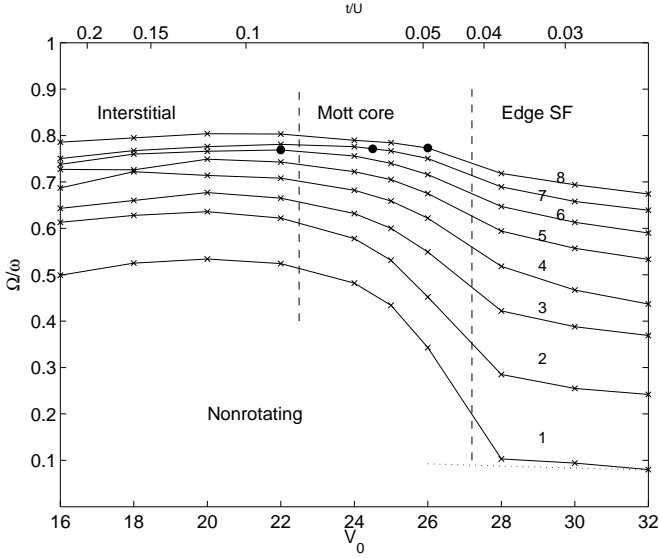


Fig. 5: Critical frequencies $\Omega_{C,q}$ for rotational states in the Hubbard model, as a function of the optical lattice potential depth V_0 . The chemical potential and external trapping potential are fixed at $\mu = 0.5U$ and $\tilde{\omega} = 0.025$. The numbers denote the total circulation of the state that is thermodynamically favorable in the indicated interval. The dotted line is the prediction of Eq. (3). The horizontal dashed lines mark the transitions between the rotational phases (see text). The dots mark the transitions between vortex lattices of different symmetry, for a total of 6, 7, and 8 quanta, respectively, in order of increasing V_0 .

shown in Fig. 5 should be supplemented with an analysis of the dynamical process for exciting vortices, but such an analysis is not attempted here.

Some features of the phase diagram can be understood quantitatively. Deep in the Mott phase, rotation results in an edge current. Since the superfluid forms an annulus around the central Mott insulating core, the energy cost for creating a circulating current – a phase winding – is small and the critical angular velocity for exciting such a current will be accordingly small. In order to estimate the critical angular velocity, assume that the rotation does not appreciably change the number of superfluid atoms, but only induces a phase winding. The superfluid atoms, whose number we denote N_C , reside in a thin shell of some thickness d whose radius is R , the size of the system. This radius is obtained from the condition that the external potential matches the chemical potential: in dimensionful units, $R^2 = 2\mu/[m(\omega^2 - \Omega^2)]$. The velocity at radius R is $v = (\hbar/m)q/R$, where q is the phase winding. The energy associated with the rotation is just equal to half the squared velocity times the number of superfluid atoms, $E_{\text{rot}} = N_C m v^2 / 2$, while the total angular momentum is $L = N_C m v R$. Hence the angular velocity for stabilization of q units of angular momentum is given by the solution

to the equation

$$\tilde{\Omega}_{C,q} = \frac{\pi \hbar}{\sqrt{2} E_R} \frac{E_{\text{rot}}}{L} = \frac{1}{\sqrt{2\pi}} q \frac{\tilde{\omega}^2 - \tilde{\Omega}_{C,q}^2}{2\mu}, \quad (3)$$

where we have returned to dimensionless units. It is seen in Fig. 5 that the estimate holds very well for the first critical frequency. However, it should be noted that the very close quantitative agreement is probably fortuitous, since the higher critical frequencies do not agree to the same level of precision.

For a Bose-Einstein condensate, it is known that all the critical frequencies should approach the trap frequency as the ratio of kinetic energy to interaction energy is increased [23]. The reason why the critical frequency does not increase as V_0 is decreased below approximately $V_0 = 20$ is that the system enters the interstitial vortex phase, where estimates for Bose-Einstein condensates cannot be trusted. Besides, this study is performed at a fixed ratio μ/U , and the total number of bosons increases as a function of V_0 at fixed $\tilde{\Omega}$. The transition between the Mott-core and interstitial vortex phases at $V_0 = 22.5$ is indicated in Fig. 5.

The solid circles in the phase diagram mark the transitions from ring configurations of vortices, for large V_0 , to lattice-like vortex arrays for smaller V_0 , as exemplified in Fig. 4. This transition is most likely due to competition between two energies. The tendency for the vortices to arrange themselves on a ring arises from the “accidental” fact that at the chosen chemical potential $\mu = 0.5$, the condensate density n_C develops a local minimum at a finite radius, which attracts the vortices. Further from the Mott transition the minimum weakens, and in combination with the repulsion between vortices it leads to the more familiar vortex lattices. By adding rotation to the already complicated phase structure of trapped bosons in optical lattices, a wealth of such different vortex configurations can be expected.

The detection of these intriguing rotating states was discussed in Ref. [10], where it was observed that time-of-flight imaging can yield quantitative information about the state. The image of the atom cloud following a release from the trap will be distinctive: the Mott insulating atoms expand incoherently, but the Bose-Einstein condensed fraction assumes a shape close to the Fourier transform of the condensate wave function z_i ; it is seen that the Fourier transform contains plenty of information on the original spatial distribution. Because of the periodic potential, copies of this image appear translated by reciprocal lattice vectors [2]. Six examples of expected time-of-flight images are shown in Fig. 6. In order to enhance contrast, the time-of-flight technique may be combined with selective removal of Mott insulating atoms [3]. Time-of-flight imaging can thus easily discriminate between vortex lattices and edge superfluids. It will also directly reveal the symmetry of the vortex lattice. The transition between interstitial and Mott-filled vortices cannot, however, be easily seen in this way. In order to spot this transition, the

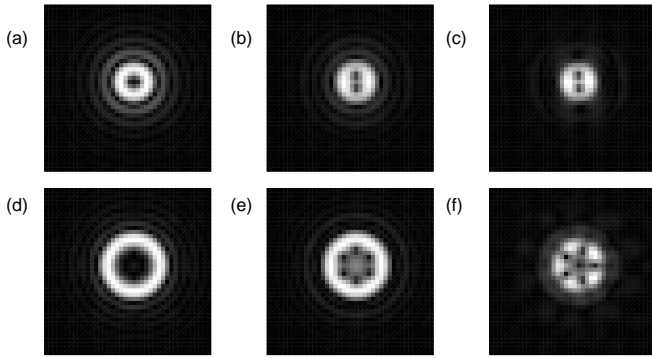


Fig. 6: Examples of density profiles after expansion of a rotating cloud. (a) is the expected time-of-flight image of the state corresponding to Fig. 1(a-c); (b) corresponds to Fig. 1(g-i); (c) corresponds to Fig. 1(j-l); (d) corresponds to Fig. 4(d-f); (e) corresponds to Fig. 4(g-i); and (f) corresponds to Fig. 4(j-l).

method of direct detection of Mott insulating sites [3, 4] should be used instead.

In conclusion, the rotating states for trapped bosons in an optical lattice have been mapped out. Three basic types of state have been identified, namely edge current, Mott-filled vortices and interstitial vortices. The transition between the two former phases coincides with the Mott transition. The transitions between the three types of state are found to be quite abrupt. Critical frequencies are calculated for low-lying rotating states. It is likely that both time-of-flight experiments and occupation-number sensitive detection are needed in order to detect the states discussed here; examples of predicted experimental signatures are calculated. Seeing that symmetries of vortex arrays are sensitive to the radial dependence of the condensate density, it is conceivable to think of vortex patterns as an experimental probe for the phase diagram of the trapped bosonic Hubbard model.

This research was conducted using the resources of High Performance Computing Center North (HPC2N), and financially supported by the Swedish Research Council, Vetenskapsrådet.

REFERENCES

- [1] JAKSCH D., BRUDER C., CIRAC J. I., GARDINER C. W. and ZOLLER P., *Phys. Rev. Lett.* , **81** (1998) 3108.
- [2] GREINER M., MANDEL O., ESSLINGER T., HÄNSCH T. and BLOCH I., *Nature* , **415** (2002) 39.
- [3] CAMPBELL G. K., MUN J., BOYD M., MEDLEY P., LEANHARDT A. E., MARCASSA L., PRITCHARD D. E. and KETTERLE W., *Science* , **313** (2006) 649.
- [4] FÖLLING S., WIDERA A., MÜLLER T., GERBIER F. and BLOCH I., *Phys. Rev. Lett.* , **97** (2006) 060403.
- [5] REIJNDERS J. W. and DUINE R. A., *Phys. Rev. Lett.* , **93** (2004) 060401.
- [6] TUNG S., SCHWEIKHARD V. and CORNELL E. A., *Phys. Rev. Lett.* , **97** (2006) 240402.
- [7] BHAT R., PEDEN B. M., SEAMAN B. T., KRAMER M., CARR L. D. and HOLLAND M. J., *Phys. Rev. A* , **74** (2006) 063606.
- [8] WU C., DONG CHEN H., PIANG HU J. and ZHANG S.-C., *Phys. Rev. A* , **69** (2004) 043609.
- [9] GOLDBAUM D. S. and MUELLER E. J., *Phys. Rev. A* , **77** (2008) 033629.
- [10] SCAROLA V. W. and SARMA S. D., *Phys. Rev. Lett.* , **98** (2007) 210403.
- [11] BURKOV A. A. and DEMLER E., *Phys. Rev. Lett.* , **96** (2006) 180406.
- [12] NIEMEYER M., FREERICKS J. K. and MONIEN H., *Phys. Rev. B* , **60** (1999) 2357.
- [13] JAKSCH D. and ZOLLER P., *New J. Phys.* , **5** (2003) 56.
- [14] OKTEL M. O., NITA M. and TANATAR B., *Phys. Rev. B* , **75** (2007) 045133.
- [15] MADISON K. W., CHEVY F., WOHLLEBEN W. and DALIBARD J., *Phys. Rev. Lett.* , **84** (2000) 806.
- [16] MATTHEWS M. R., ANDERSON B. P., HALJAN P. C., HALL D. S., WIEMAN C. E. and CORNELL E. A., *Phys. Rev. Lett.* , **83** (1999) 2498.
- [17] RAMAN C., ABO-SHAER J. R., VOGELS J. M., XU K. and KETTERLE W., *Phys. Rev. Lett.* , **87** (2001) 210402.
- [18] ANDERSEN M. F., RYU C., CLADE P., NATARAJAN V., VAZIRI A., HELMERSON K. and PHILLIPS W. D., *Phys. Rev. Lett.* , **97** (2006) 170406.
- [19] BHAT R., PEDEN B. M., SEAMAN B. T., KRAMER M., CARR L. D. and HOLLAND M. J., *Phys. Rev. A* , **74** (2006) 063606.
- [20] SACHDEV S., *Quantum Phase Transitions* (Cambridge University Press, Cambridge) 1999.
- [21] ELSTNER N. and MONIEN H., *Phys. Rev. B* , **59** (1999) 12184.
- [22] BERGKVIST S., HENELIUS P. and ROSENGREN A., *Phys. Rev. A* , **70** (2004) 053601.
- [23] PETHICK C. and SMITH H., *Bose-Einstein Condensation in Dilute Gases* (Cambridge University Press, Cambridge) 2002.
- [24] FETTER A. L., *Annals of Physics* , **70** (1972) 67.
- [25] SHESHADRI K., KRISHNAMURTHY H. R., PANDIT R. and RAMAKRISHNAN T. V., *Europhysics Letters* , **22** (1993) 257.
- [26] ROKHSAR D. S. and KOTLIAR B. G., *Phys. Rev. B* , **44** (1991) 10328.
- [27] LUNDH E., *Phys. Rev. A* , **65** (2002) 043604.
- [28] FETTER A. L., *Phys. Rev.* , **138** (1965) A429.
- [29] RECATI A., ZAMBELLI F. and STRINGARI S., *Phys. Rev. Lett.* , **86** (2001) 377.